Unravelling the Role of Oxygen Vacancies in the Mechanism of the Reverse Water-Gas-Shift Reaction by *Operando* DRIFTS and UV-Vis Spectroscopy

Luis F. Bobadilla †,, José L. Santos †, Svetlana Ivanova †, José A. Odriozola † and Atsushi Urakawa ‡*

† Instituto de Ciencia de Materiales de Sevilla, Centro Mixto CSIC-Universidad de Sevilla, Av. Américo Vespucio 49, 41092 Sevilla, Spain

‡ Institute of Chemical Research of Catalonia (ICIQ), The Barcelona Institute of Science and Technology, Av. Països Catalans 16, 43007 Tarragona, Spain

ABSTRACT

The reaction mechanism of reverse water-gas shift (RWGS) reaction was investigated using two commercial gold-based catalysts supported on Al_2O_3 and TiO_2. The surface species formed during the reaction and reaction mechanisms were elucidated by transient and steady-state *operando* DRIFTS studies. It was revealed that RWGS reaction over Au/Al_2O_3 proceeds through the formation of formate intermediates that are reduced to CO. In the case of Au/TiO_2 catalyst, the reaction goes through a redox mechanism with the suggested formation of hydroxycarbonyl intermediates, which further decompose to CO and water. The Ti^{3+}species, the surface hydroxyls,

and oxygen vacancies jointly participate. The absence of carbonyl species adsorbed on gold particles during the reaction for both catalysts indicates that the reaction pathway involving dissociative adsorption of CO_2 on Au particles can be discarded. To complete the study *Operando* UV-Vis spectroscopy was successfully applied to confirm the presence of Ti^{3+} and to understand the role of the oxygen vacancies of TiO_2 support in activating CO_2 and thus the subsequent RWGS reaction.

KEYWORDS. *RWGS; Au-based catalysts; Operando; DRIFTS; UV-Vis*

1. INTRODUCTION

During the last decade increasing interests have been witnessed in developing novel catalytic technologies and processes to utilize carbon dioxide as a C1 building block for the synthesis of valuable chemicals and fuels [1]. Among available options, hydrogenation of CO_2 is one of the most intensively investigated reactions for the broad product scope. Various commercially important products, from C1 molecules (CH_4, CH_3OH) to higher molecular weight hydrocarbons and alcohols through C–C bond formation, can be produced by CO_2 hydrogenation [2]. Particularly, reverse water-gas shift (RWGS) reaction ($CO_2 + H_2 \rightleftarrows CO + H_2O$) is considered as the key step in the catalytic hydrogenation of CO_2 to produce chemical fuels, since the established industrially important syngas-based reactions (e.g. Fischer-Tropsch and methanol synthesis reactions) become within reach [3]. It is therefore obvious that developing more efficient catalysts and understanding the nature of catalysts under RWGS conditions are of fundamental importance.

Pioneered by Haruta [4], Au-based catalysts are well known for their high catalytic activity in the water-gas shift (WGS) and RWGS reactions when Au is highly dispersed on support materials [5-

[12]. Support material can influence the electronic properties of active metal centers and it can participate directly in the reaction by interacting with the reactants. It has been proposed that activation of CO_2 occurs at the oxide support or the interfacial sites between the active metal and the oxide support [13]. Through a combined experimental and theoretical study, Yang et al. [14] demonstrated that an electronic polarization at the metal−oxide interface of Au nanoparticles anchored and stabilized on a CeO_x/TiO_2 substrate generates active centers for CO_2 adsorption and its low pressure hydrogenation, leading to an optimal catalytic performance. They found that reduced oxides have a strong tendency to activate the CO_2 even causing direct C-O bond scission. Thus, a proper tuning of Au-oxide interface can promote the hydrogenation of CO_2. However, there are still controversies with regard to the effects of support and it roles on the activity of supported gold catalysts.

Generally, two major mechanisms are suggested for RWGS reaction; the regenerative redox mechanism and the associative one. In the redox mechanism, hydrogen is proposed to be a reducing agent without direct participation in the formation of intermediates in RWGS reaction. Normally the support is of reducible nature [15]. The validity of the redox mechanism is based on the fundamental assumption that CO_2 can efficiently re-oxidize the partially reduced support at low temperatures leading to the formation of CO. On the other hand, the associative mechanism suggests that CO is formed from formate intermediates decomposition, derived from the association of hydrogen with CO_2. Since the formate intermediates cannot be decomposed on Au nanoparticles, their transformation is strongly influenced by the support, according to a report [16]. In addition to the main redox and associative mechanisms, other authors proposed the so-called carbonate mechanism for the RWGS reaction [17-18]. For instance, Millar et al. [17] suggested this mechanism over Cu/SiO_2 catalyst based on a combined temperature programmed desorption

(TPD) and infrared (IR) study of CO_2 and H_2 interactions. They found that increasing the availability of activated surface symmetric carbonate species induced an increase in the formation of formate species, stable intermediates in the methanol synthesis or the decomposition to CO and water.

Monitoring the surface phenomena occurring over catalyst under reaction conditions is essential to elucidate the relevant reaction steps, active sites and intermediates as well as to establish the relationships between catalytic performance (reactivity/selectivity) and structure of the solid. This knowledge is of great importance for the rational catalyst design and to improve their catalytic properties for specific applications [19]. IR spectroscopy is a very useful technique to identify the adsorbed species and elucidate the reaction mechanisms in heterogeneously catalyzed reactions. Nevertheless, IR spectroscopy has serious drawbacks such as the complexity to distinguish reactive intermediates from spectators. IR spectroscopy may be combined with other characterization techniques such as EPR, NMR, Raman, UV-Vis and XAFS, or integrated with an optical microscope to analyze heterogeneities within and between catalyst grains. On the other hand, UV-Vis spectroscopy is a powerful method for electronic structure studies as it can probe, for example, the electronic *d–d* transitions for transition metals if present in the catalysts [20]. For instance, Gonzalez-Castaño et al. [7] investigated the influence of the support over Au and Pt catalysts in WGS reaction by means of UV-Vis spectroscopy and they found that the catalytic performance is directly correlated with the electronic properties of the metal/support interactions.

Herein, we investigated the possible pathways for CO formation in the RWGS reaction focusing our attention on the role played by the support material over highly dispersed Au catalysts. For this purpose, we selected two model supports: a non-reducible (Al_2O_3) and a reducible (TiO_2) one.

The differences in the reaction mecanism over the different nature oxides were studied by *operando* DRIFTS and UV-VIS spectroscopy.

2. EXPERIMENTAL SECTION

2.1. Materials and characterization

The catalysts used in this investigation were the commercially available materials (AUROlite™) consisting of 1 wt.% of ca. 2.0 nm Au particles supported on TiO_2 and Al_2O_3 supplied by STREM in collaboration with Project AuTEK [21].

We employed powder X-ray diffraction (XRD) to analyse the structure of the two Au supported catalysts (see Figure S1 in the Supporting Information). The gold particles size and morphology were studied by Transmission Electron Microscopy (HR-TEM) on a FEI Talos electron microscope using an acceleration voltage of 200 kV with a field emission filament and a side mounted Ceta 16M camera. A standard holey carbon-covered copper TEM grid was used for supporting the catalyst. The average gold particle size for both fresh and spent catalysts, was estimated considering around 200 particles as follows:

$$D_p = \frac{\sum n_i d_i^3}{\sum n_i d_i^2} \qquad \text{(Eq. 1)}$$

where n_i represents the number of particles with diameter d_i.

2.2. Catalytic testing

The catalytic activity of the gold catalysts in CO_2 hydrogenation was measured using a tubular fixed-bed flow reactor (3.4 mm inner diameter) made of stainless steel. The catalyst (200 mg) was sieved to the range of 200-300 μm and then loaded in the reactor. Before testing, the fresh catalyst

was pre-treated at 250 °C for 1 h using a feed that contained 10 vol.% H_2 in He to reduce and remove moisture from the sample. Then, the reaction mixture was introduced into the reactor using a flow rate of 50 mL min^{-1} (5 mL min^{-1} CO_2 and 20 mL min^{-1} H_2, H_2/CO_2 molar ratio of 4) and GHSV of 12,000 h^{-1} for Au/Al_2O_3 and 12,000 – 40,000 h^{-1} range for Au/TiO_2. The temperature was increased to 450 °C in 25 °C increments and was held constant at each setting for 30 min to ensure the stable isothermal activity. The effluent gas stream was passed into a transmission gas cell of an IR spectrometer (Bruker ALPHA) for quantitative product analysis and estimation of CO_2 conversion. CO was the only observed product.

2.3. *Operando* DRIFTS measurements

Operando DRIFTS experiments were carried out using a reaction chamber (HVC-DRP, Harrick) mounted in a Praying Mantis (Harrick) DRIFTS optical system equipped with ZnSe windows. The spectra were collected in the range 650-4000 cm^{-1} using a Bruker Vertex 70V FTIR spectrometer equipped with an MCT detector. About 50 mg of catalyst was placed in the cell for each measurement. The flow of gases was controlled by means of mass flow controllers (Bronkhorst). The gases pass through the sample (catalyst) packed-bed, mimicking the plug-flow condition of the reaction. Prior to each measurement, catalyst was pre-treated *in situ* at 250 °C in H_2 diluted in He stream (5 ml min^{-1} H_2 and 45 ml min^{-1} He) for 1 h.

To gain insights into the evolution of surface species over the Au catalysts, transient experiments were performed by alternatingly passing 20% H_2 in He and 5% CO_2 in He at 10 mL min^{-1} for sufficiently long times to stabilize the DRIFTS signal. A four-way switching valve (VICI, 2 position and 4 port switching valve) was used to select the CO_2 or H_2-containing streams. On the other hand, the reaction of CO_2 hydrogenation was performed by passing 20% H_2 and 5% CO_2 in

He (H_2/CO_2 = 4 molar ratio) at 10 mL min^{-1}. The spectra were recorded every 30 seconds to follow the reaction and stabilization process of the surface species. Both experiments were carried out at the starting temperature of the catalytic test (250 ºC), where the level of product formation was low and all surface species unstable at high temperatures can be more clearly observed. The effluent gas stream was analyzed on line by the IR spectrometer (Bruker ALPHA).

2.4. *Operando* UV-Vis spectroscopy

The catalytic cell used in the *operando* UV-Vis study is a modified version of the commercial CCR1000 reactor cell from Linkam Scientific Instruments (Figure 1). A high-temperature reflection UV-Vis probe formed by six radiating optical fibers and one reading fiber was located inside the reactor cell above the catalytic bed to analyze the optical properties of the sample. The experimental device allows to heat the sample under desired atmosphere and the gas effluents are analyzed on-line by mass spectrometry (MS). In contrast to the generally used cell reactors with spectroscopic quartz windows [22-23], our catalytic cell does not use any window and the cell is sealed by O-rings. Figure 1 includes a 3D schematic representation (Figure 1) of the catalytic cell. The sample (about 50 mg) is positioned in a ceramic holder on a fiber filter and the reaction gas mixture is passing through it from the top to the bottom of the catalytic bed. The temperature is controlled by a Linkam TMS94 temperature controller.

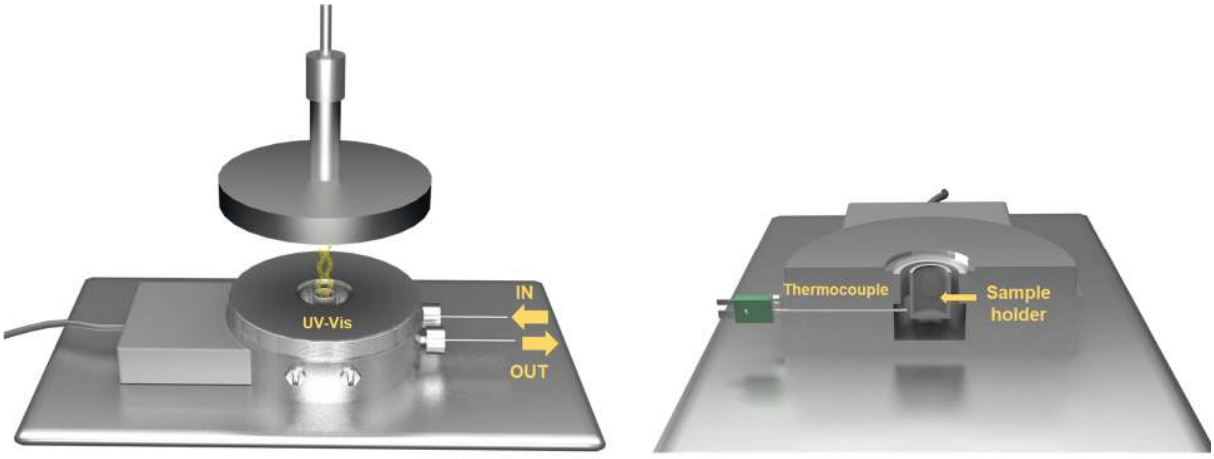

Figure 1. 3D schematic representation of *operando* UV-Vis spectroscopic cell for catalyst characterization under reaction conditions.

Operando UV-Vis experiments were performed under steady-state conditions in the range of λ = 200 – 1000 nm using an AVASPEC fiber optical spectrometer (Avantes) equipped with a DH-2000 deuterium-halogen light source and a charge coupled device (CCD) array detector. Barium sulfate was used as a white reference material. The UV-Visible spectra were recorded at room temperature on a fresh sample and during the reduction treatment (total flow of 50 mL min^{-1} of 10% H_2 in He) at 250 ºC for 1 h and RWGS reaction (total flow of 50 mL min^{-1} of H_2/CO_2/He = 32/8/60) in the 150-450 ºC temperature interval after stabilizing the gas flows and temperature. The spectra are presented either in absorbance (A) mode or in difference spectral mode, with the latter highlighting the spectral changes during catalytic reaction. If A1 and A2 are the spectra before and after the sample treatment a difference (A2-A1) > 0 corresponds to treatment induced absorption and, if negative, disappearance of already existing light absorbing entities.

2.5. Oxygen storage complete capacity (OSCC) measurements

Oxygen Storage Complete Capacity (OSCC) of the samples was measured over 50 mg of sample loaded in U-shaped reactor. The samples were pretreated in Ar flow at 350 ºC for 1 h and the temperature decreased to the first studied temperature (150 ºC) at which the oxygen storage capacity was measured. Once the temperature stabilized, ten O_2 pulses of 1 mL each were injected every 2 min followed by ten CO pulses. The OSCC was calculated by the formed CO_2 during the CO pulses. This experiment allows to calculate the stoichiometric coefficient for TiO_x, where x falls within the 1.5 - 2 range, with the first value corresponding to the presence of reduced (Ti^{3+}) only and the last value to completely oxidized (Ti^{4+}) titanium ion. From this value, the degree of reduction of Ti^{4+} to Ti^{3+} could be elucidated.

3. RESULTS AND DISCUSSION

3.1. Steady-state activity measurements

Figure 2 shows the RWGS CO_2 conversion as a function of the reaction temperature for Au/Al_2O_3 and Au/TiO_2. The CO_2 conversion increased with the temperature for both catalysts. No products other than CO were observed, although the formation of traces of alcohols or other oxygenated compounds formed below our detection limit cannot be ruled out. Compared to Au/Al_2O_3, Au/TiO_2 catalyst exhibited higher RWGS activity, reaching values close to the thermodynamic limit. To ensure the kinetic regime of the reaction, the space velocity (GHSV) was increased to 40,000 h^{-1} for Au/TiO_2, showing lower CO_2 conversion due to the decrease of the reactants residence time.

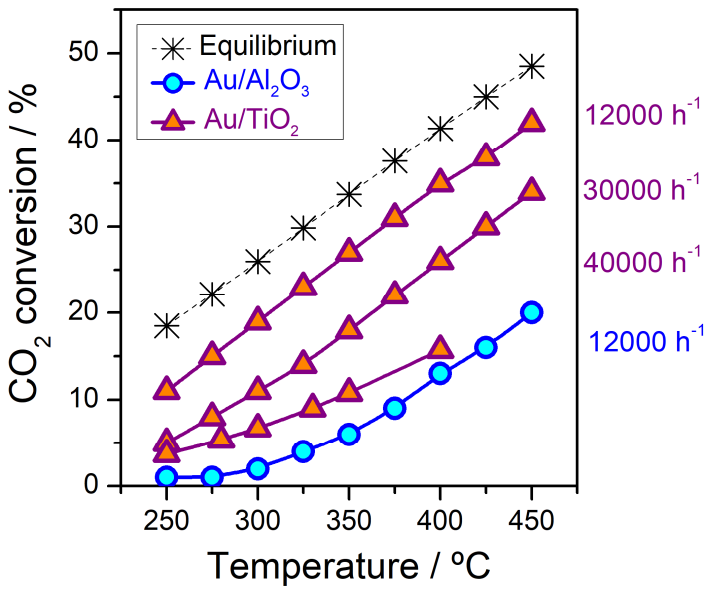

Figure 2. Catalytic performance of Au/TiO_2 and Au/Al_2O_3 catalysts in RWGS reaction (H_2/CO_2 molar ratio = 4)

As the gold particles size could play a very important role in the catalytic performance, the possible gold particle state changes were investigated by HR-TEM (Figure 3). The mean particle size of the fresh catalysts was slightly larger than stated by the supplier, 2.7 and 3.5 nm were observed for Au/Al_2O_3 and Au/TiO_2 respectively. The gold particles may have sintered during the catalyst storage. The average particle size of the catalysts was found even bigger after reaction resulting in sizes rounding 5 nm for both catalysts. This indicates that during the reaction and/or catalyst pretreatment sintering of the gold nanoparticles occurs. This behavior was also found by Walther et al. [24] for the same catalyst in reactions of CO and H_2 oxidation. However, the conversion up/down was identical even reaching maximal temperature of 400 ºC (Figure S2).

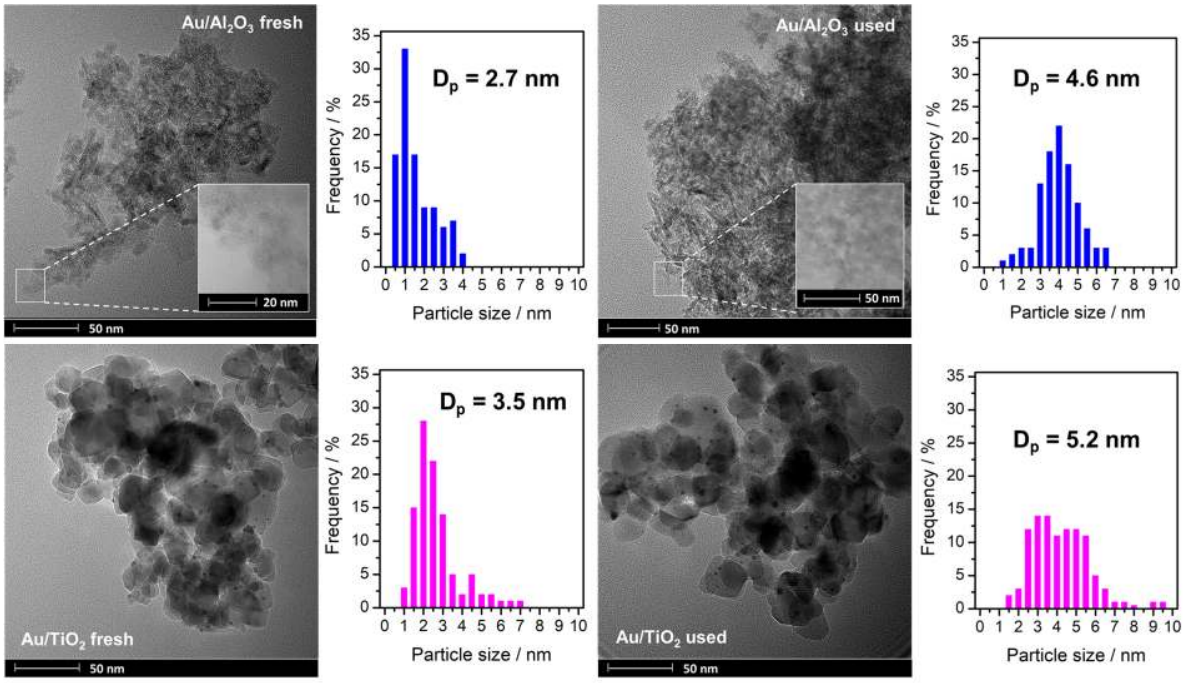

Figure 3. TEM micrographs of the fresh and spent catalysts with their corresponding statistical analysis of the mean particle size.

The catalytic activity was also evaluated in terms of turnover frequency (TOF), which was calculated by using the following equation [11]:

$$TOF = \frac{r}{D_{Au}} \ [s^{-1}] \qquad \text{(Eq. 2)}$$

where r is the reaction rate expressed in $mol_{co\ produced}\ mol_{Au}^{-1}\ s^{-1}$ and D_{Au} is the metal dispersion. Gold dispersion was calculated on the basis of a hemispherical ball model assuming the average Au particle size estimated by TEM (Figure 3) for the spent catalysts. The dispersion discloses the total number of gold atoms accessible for the RWGS reaction. Figure 4 shows TOFs plotted against the reciprocal temperature expressed in Kelvin unit in order to estimate the apparent activation energy (E_{act}). To approximate differential conditions, the estimated rate values were determined in the 5–20% range of CO_2 conversion. The apparent activation energy obtained for Au/TiO_2 (30 kJ

mol^{-1} – 0.30 eV) was very different from that of Au/Al_2O_3 (79 kJ mol^{-1} – 0.79 eV). Since the Au loading and the average particle size, consequently the Au dispersion, for both catalysts are similar, the results obtained for the activation energy clearly indicate that the reaction rate does not straightforwardly relate to the Au particles state. As the only difference for the systems is their support nature, it is fair to suppose that the support participates very actively in the reaction. Also the differences found in the activation energy suggests distinct rate-determining steps for Au/TiO_2 and Au/Al_2O_3. Very similar observation was reported by Shetkar et al. [12] when studying the WGS reaction. They demonstrated that Au nanoparticles supported on TiO_2 showed higher catalytic rates than those supported on Al_2O_3 and relate it to the fact that the support directly participates in the H_2O molecules activation. Numerous studies propose that the reason for the notable activity enhancement registered for reducible-oxide supported catalysts (as TiO_2) is due to the direct participation of the support in the reaction through redox or formate mechanism [5, 7, 25-27]. To unravel the effect of support material on the reaction mechanisms and the catalytic performance, we performed *operando* spectroscopic investigations under RWGS reaction conditions over both Au catalysts.

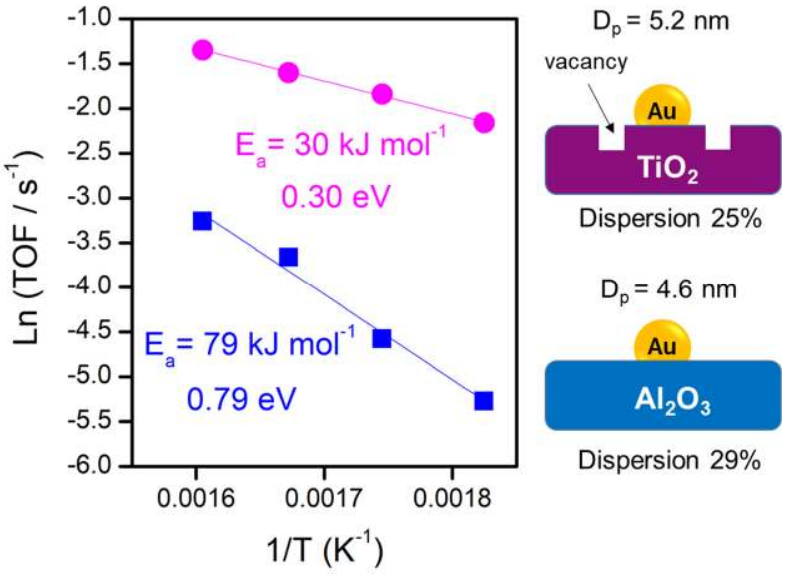

Figure 4. Arrhenius plot for the Au/Al_2O_3 and Au/TiO_2 catalysts in RWGS reaction

3.2. *Operando* transient and steady-state DRIFTS measurements

DRIFTS experiments under transient conditions were performed to investigate the surface species formed over Au/TiO_2 and Au/Al_2O_3 catalysts under *operando* conditions. We examined the formation of surface species at 250 ºC under the gas stream containing 5% CO_2 in He, and subsequently, by switching to 20% H_2 in He. The gas-phase was monitored by coupling to an IR spectrometer equipped with a transmission gas cell. Prior to the measurements, the catalysts were activated in 10% H_2 in He for 1 h at 250 ºC and then stabilized in He to ensure the complete removal of adsorbed and/or absorbed hydrogen species.

A series of DRIFT spectra recorded during CO_2 exposure and subsequent reaction in H_2 flow over Au/Al_2O_3 catalyst are presented in Figure 5. The IR bands emerged during the CO_2 exposure can be assigned exclusively to adsorbed species on alumina support since no CO adsorbed species were observed on the gold particles. The spectral features developed at 1229, 1437 and 1647 cm^{-1} clearly evidences the formation of surface bicarbonates [28]. The bicarbonates are generated from the reaction between CO_2 and the hydroxyl groups on the Al_2O_3 support. After switching from CO_2 to H_2 stream, the bicarbonate bands gradually decreased while new bands appeared at 1372, 1392 and 1590 cm^{-1}, which are attributed to adsorbed formate species on alumina [29-30]. It is evident from the presence of an isosbestic point at about 1600 cm^{-1} that bicarbonates transform into formate species at 250 ºC. It has been reported that in the reaction of CO_2 hydrogenation on Pd/Al_2O_3 and Ru/Al_2O_3, bicarbonates are intermediates to the formates via the reaction with adsorbed H species on noble metal particles[30-31]. Our results suggest that probably the same mechanism for bicarbonates to formate species conversion is also valid for Au/Al_2O_3. Gold is

typically considered inactive for the H_2 dissociation. However, it has been demonstrated that small gold particles may present a peculiarly high activity [27]. Since Al_2O_3 cannot activate H_2 under the investigated conditions, Au should participate in the H_2 activation in a dissociative manner, being the produced H species spilled over to the Al_2O_3 surface thus reducing the bicarbonates to formates.

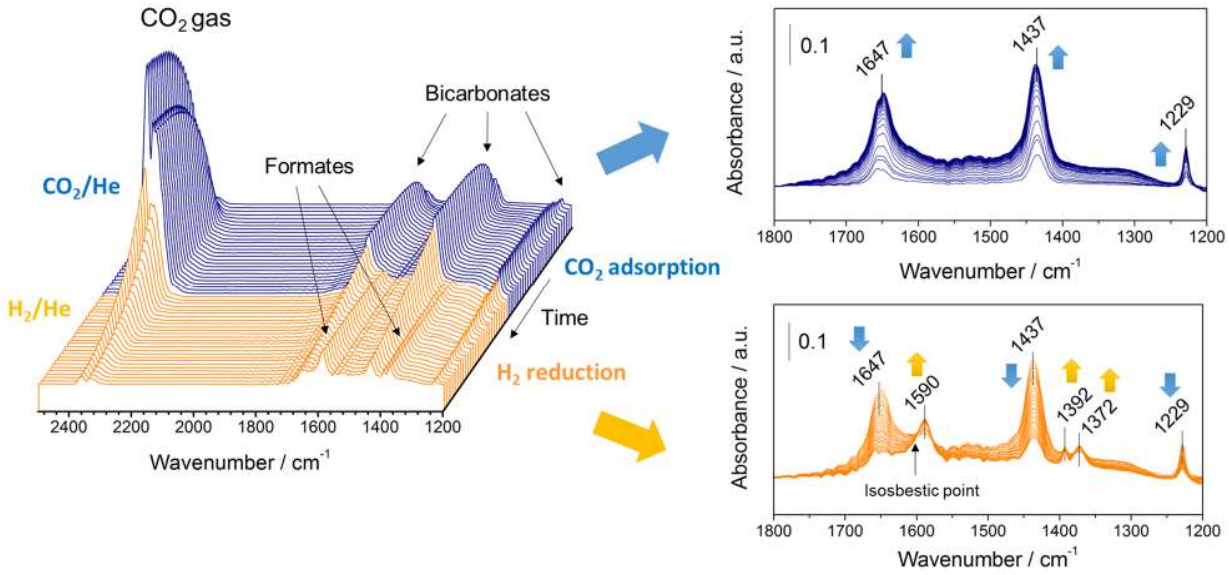

Figure 5. Transient DRIFT spectra collected at 250 ºC where the feed gas was switched from 5% CO_2 to 20% H_2 (both in He) over Au/Al_2O_3. Pretreatment condition: 250 °C in H_2 diluted in He stream (5 ml min^{-1} H_2 and 45 ml min^{-1} He) for 1 h

The identical experiment was performed for Au/TiO_2 and the results are shown in Figure 6. Several spectral features in the range of 1300-1650 cm^{-1} assigned to carbonates, carboxylates and formate species adsorbed on TiO_2 support were observed. The band at 1527 cm^{-1} is characteristic of the C=O stretch vibration of bidentate carbonates whereas the feature appearing at 1430 cm^{-1} is commonly assigned to asymmetric stretching vibration ν_{as} (COO) of monodentate carbonates [32]. The band with minor intensity observed at 1620 cm^{-1} is typical of carboxylate species [33]. The bands

at 1556 and 1360 cm^{-1} gradually emerged and they can be attributed to formate species on the TiO_2 surface [32, 34]. These emergence of the two bands were accompanied by those of two weak bands at 2950 and 2870 cm^{-1} (not shown) that were assigned to ν_{CH} of formate species [35]. No band was observed around 1220-1250 cm^{-1} indicating the absence of bicarbonates species. It should be stressed that bicarbonates could be formed and very rapidly reduced to formates in the presence of vacancies and this process requires hydrogen [36]. In our experimental conditions we observe the formation of CO and it is well known that hydrogen can be produced by the reaction between CO and hydroxyl species on the support [37]. Early studies on the interaction of CO with the surface of Rh/ZrO_2 catalysts have shown that CO adsorbed on Rh sites may react with surface hydroxyls groups of zirconia resulting in the formation of adsorbed formate species [38]. Moreover, Senayaje et al. [39] also suggested this hypothesis discarding the decomposition of formate species as hydrogen source upon interaction of CO with hydroxyl groups. Following the reaction mechanisms typically postulated in the study of the WGS, it is possible to ensure that the reaction of hydroxyls groups with CO can produce formate, carboxyl, and/or carbonate species as key intermediates before the final production of CO_2 and H_2 [40]. After switching to H_2 flow, gaseous CO was detected and the signals of formate and carbonate species disappeared gradually, which indicated that these species formed over Au/TiO_2 are the main intermediates for CO formation. Presumably, surface formates and carbonates species are initially formed at the $Au–TiO_2$ interface and they subsequently migrated to more stable locations on the TiO_2 support.

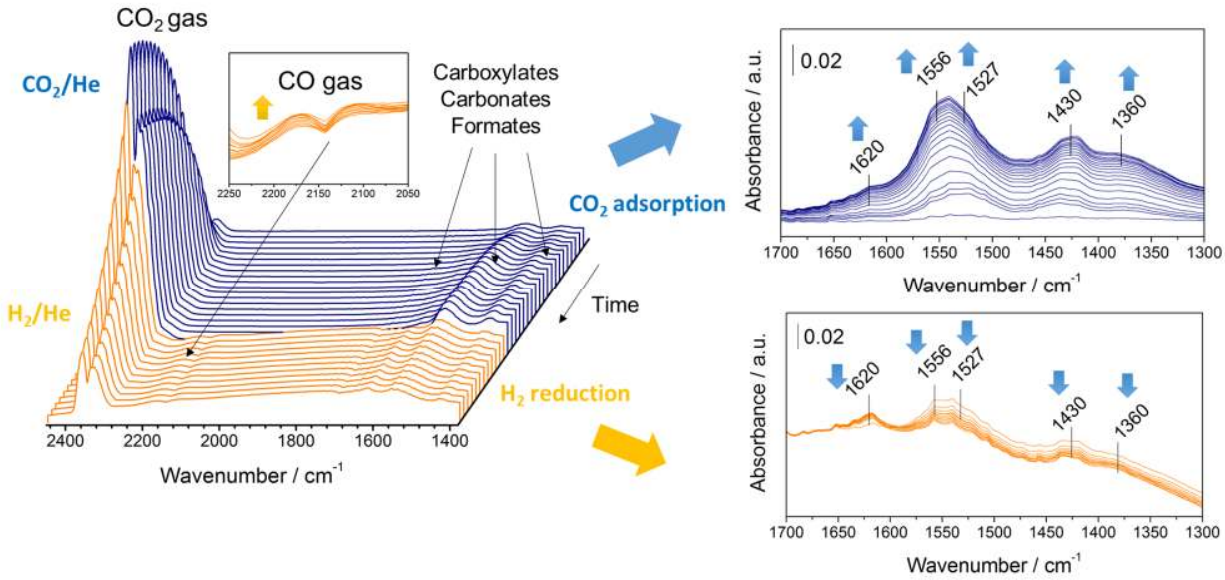

Figure 6. Transient DRIFT spectra collected at 250 ºC where the feed gas was switched from 5% CO_2 to 20% H_2 (both in He) over Au/TiO_2. Pretreatment condition: 250 °C in H_2 diluted in He stream (5 ml min^{-1} H_2 and 45 ml min^{-1} He) for 1 h

In order to gain further insights into the reaction intermediates leading to CO formation, surface species during RWGS (i.e. the mixture of CO_2 and H_2) at 250 ºC was studied by DRIFTS (Figure 7A-B). CO_2 was initially adsorbed over Au/Al_2O_3, forming surface bicarbonate species via the reaction of CO_2 with surface OH groups. The H_2 dissociation, which takes place on gold, results in the formation of Au-H species that attack surface bicarbonates forming adsorbed formate species. Figure 7C displays the evolution of the band intensities for the bicarbonate and the formate species with the reaction time evidencing a close correlation between both species. These data clearly reveal that formates are directly formed from bicarbonate reduction assisted by hydrogen. The formate species are finally decomposed to CO and the reaction follows clearly the associative mechanism over Au/Al_2O_3.

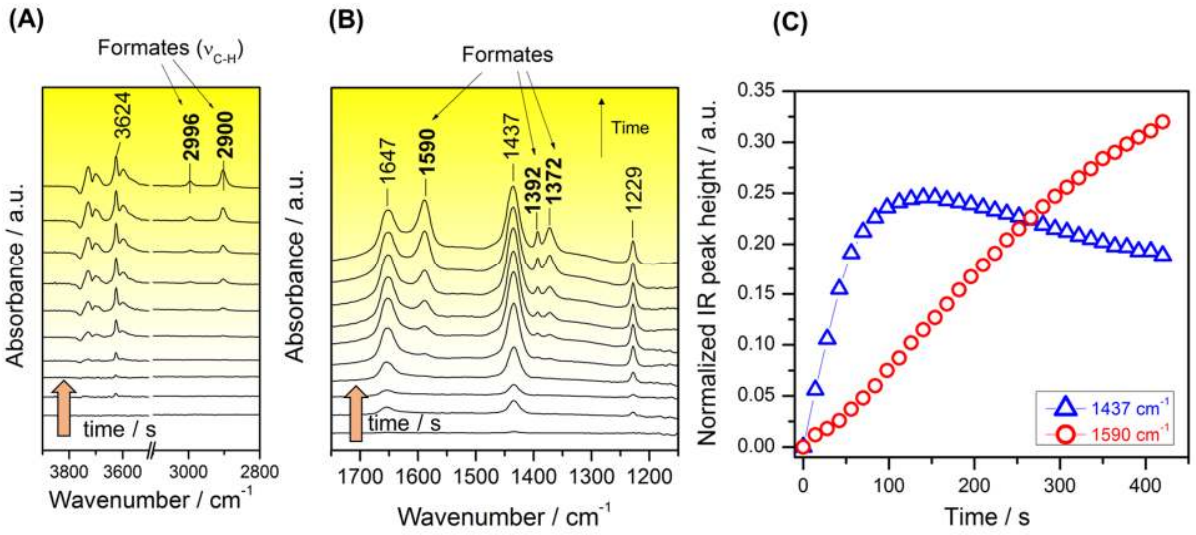

Figure 7. (A-B) Evolution of DRIFT spectra during RWGS reaction at 250 ºC and (C) evolution of the band height attributed to bicarbonates (1437 cm^{-1}) and formate (1590 cm^{-1}) surface species on Au/Al_2O_3 as a function of the time on stream. Pretreatment condition: 250 °C in H_2 diluted in He stream (5 ml min^{-1} H_2 and 45 ml min^{-1} He) for 1 h, and reaction conditions: 20% H_2 and 5% CO_2 in He (H_2/CO_2 molar ratio = 4) at 10 mL min^{-1}.

For CO_2 hydrogenation over Au/TiO_2 (Figure 8A-B), surface carbonate and formate species were observed as possible intermediates leading to CO and water. A closer look in the region of hydroxyl groups (3500-3700cm^{-1}) shows that a band feature at 3675 cm^{-1}, attributed to terminal hydroxyl groups associated to Ti^{4+} [41], evolved with a distinct kinetics. Figure 8C shows the trends of the intensities for hydroxyls group associated to Ti^{4+}, carbonates, and gaseous CO produced with the reaction time. Obviously, the formation of Ti^{4+}, carbonates and CO (g) are well correlated. In contrast, formates are accumulated over time. It has been reported that at low temperatures (150-200 ºC) most formates observed by IR are spectator species although this does not preclude the possibility that there are some formates involved in the reaction. As the temperature is increased, this formate path may become more probable [26]. In a study about the reaction mechanism of dry

reforming of methane, Lercher et al. [42] proposed that the main route of CO_2 hydrogenation occurs via initial formation of carbonate close to the metal-support boundary. Carbon on the metal reduces the carbonate to formate by forming CO and the formate decomposes rapidly to CO and a surface hydroxyl group that recombines to form water. Our data suggest that CO_2 is adsorbed over the titania accompanying surface oxidation from Ti^{3+} to Ti^{4+} and forming carbonates and formates that are decomposed to CO. As discussed above, CO_2 likely reacts with the hydroxyl groups with a neighbor oxygen vacancy producing unstable bicarbonates species that are rapidly reduced to formates. The absence of carbonyl species adsorbed on gold particles during the transient and steady-state experiments for both catalysts indicates that the reaction pathway involving the dissociative adsorption of CO_2 on Au particles followed by the desorption of surface CO to the gas phase can be ruled out. A reaction scheme involving CO_2 adsorption on the support and subsequent reduction to gaseous CO assisted by the active dissociated hydrogen on the metal-support interface more reasonably explain our experimental results. Similar mechanism is reported by Rodríguez et al. [43] for a CeO_x/Cu(111) sample. They proposed a mechanism in which CO_2 is hydrogenated yielding a hydroxycarbonyl intermediate (OCOH) with a relatively small calculated energy barrier (40 kJ mol^{-1}). This intermediate is easily decomposed into CO and OH, that subsequently produce water from reaction from adsorbed H and OH species. The presence of this route can not be discarded since the hydroxycarbonyl species are much more reactive than formate and carbonates, especially at lower temperatures [43].

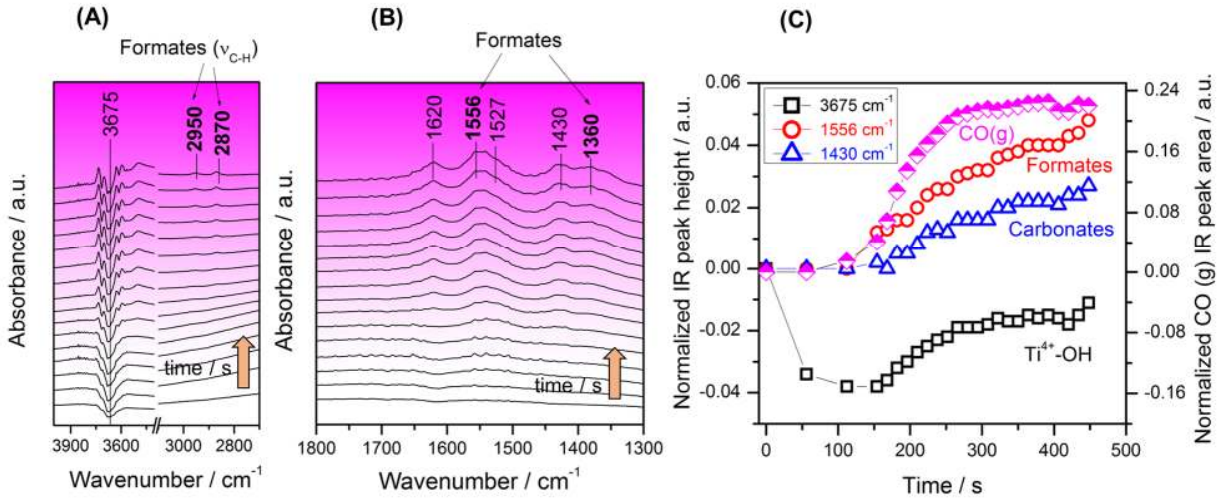

Figure 8. (A-B) Evolution of DRIFT spectra during RWGS reaction at 250 ºC, and (C) evolution of the band height attributed to Ti(IV)-OH, carbonates and formate surface species on Au/TiO_2 as well as the band area of gaseous CO as a function of the time on stream. Pretreatment condition: 250 °C in H_2 diluted in He stream (5 ml min^{-1} H_2 and 45 ml min^{-1} He) for 1 h, and reaction conditions: 20% H_2 and 5% CO_2 in He (H_2/CO_2 molar ratio = 4) at 10 mL min^{-1} and 250 ºC

The above differences in RWGS catalytic activity can be attributed to the difference in interaction of CO_2 with the supports. When the interaction of CO_2 with the support is very strong, it is considered to cause low conversion of CO_2 due to the high stability of the adsorbed species. However, the presence of the oxygen vacancies on the support may enhance the formation of surface carbonate intermediates which is further easily transformed into CO and water regenerating the initial oxidation state on the support to initiate a new redox cycle. The adsorption of CO_2 on titania leads to the formation of different types of carbonate-like species. The facile formation and subsequent reduction of these species on titania can be attributed to its electronic and defect structure. It is well known that TiO_2 in its reduced form contains a high concentration of oxygen vacancies and CO_2 could be activated on these sites through an electron transfer from

Ti^{3+} to CO_2 adsorbed [44]. In order to demonstrate the importance of the oxygen vacancies generated through the reduction of Ti^{4+} to Ti^{3+} of the support we have performed an *operando* UV-Vis spectroscopic study.

3.3. *Operando* UV-Vis spectroscopy

Figure 9A presents the UV-Vis spectra of Aeroxide® TiO_2 P25 during activation in 10% H_2 and under RWGS reaction conditions. At room temperature (dashed line) the sample shows only one absorption band at around 320 nm corresponding to the absorption edge of the valence to conduction band transfer of semiconducting TiO_2. During the activation in H_2 a spectral change appears as a broad band in the 400-800 nm range. Liu et al. [45] reported three types of interactions between H_2 and TiO_2 at different temperatures. Below 300 ºC, H_2 interacts weakly with the lattice whereas when the temperature rises the electrons are transferred from the H atoms to the lattice oxygen of titania and its vacancies are formed with H_2O release. The formation of Ti^{3+} ions are suggested above 250 ºC when electrons are transferred from the oxygen vacancies to Ti^{4+} ions. Further increase of temperature leads to $Ti^{4+} \rightarrow Ti^{3+}$ conversion rate increase, and higher relative quantity of Ti^{3+} and oxygen vacancies. The titania reduction could be also promoted by the UV irradiation [46]. However this possibility has been excluded as the UV-Vis spectra in absence of H_2 were different, allowing to assume that the reduction of titania is provoked solely by H_2. It was reported that upon reduction the titania crystals, more precisely the rutile ones, displayed very broad absorption signal ranging from 400 to 1000 nm with poor spectral features and originated from a variety of coexisting intrinsic bulk and surface defects, identified as neutral singly and doubly charged oxygen vacancies and trivalent and tetravalent Ti interstitials at different structural positions[47]. All these defects result in three superposed bands in the 400-700 nm range without clear "type defect/band" attribution. The *d-d* transitions of the Ti^{3+} ions could also be present when

the number of Ti^{3+} sites becomes significant and should appear in the long wavelength region (> 700 nm). In any case, the appearance of the broad band at 400-700 nm unequivocally suggests the presence of oxygen defects on titania. Considering the literature indications and the observed spectral features for the TiO_2 P25 sample under reduction treatments at 250 ºC (Figure 9A, orange spectra), the formation of defects attributed to oxygen deficient sites and Ti^{3+} sites are evident. The same material under the RWGS reaction condition (Figure 9A, blue spectra) did not show significant spectral changes till 350 ºC when RWGS starts taking place with CO evolution. The difference spectra (Figure 10A) demonstrates an increasing formation of defect sites under the RWGS gas mixture upon heating up to 300 ºC, supported by the changes registered in the 400-800 nm region and also by the intensity increase of a positive band at around 350 nm suggesting a bandgap modification caused probably by the contribution of the formed Ti^{3+} levels. When the temperature rises to 350 ºC, the TiO_2 starts to convert CO_2 and H_2 into CO and H_2O and the defect bands disappear as confirmed by the negative contribution in the 400-800 nm range suggesting the direct participation of these sites in the reaction.

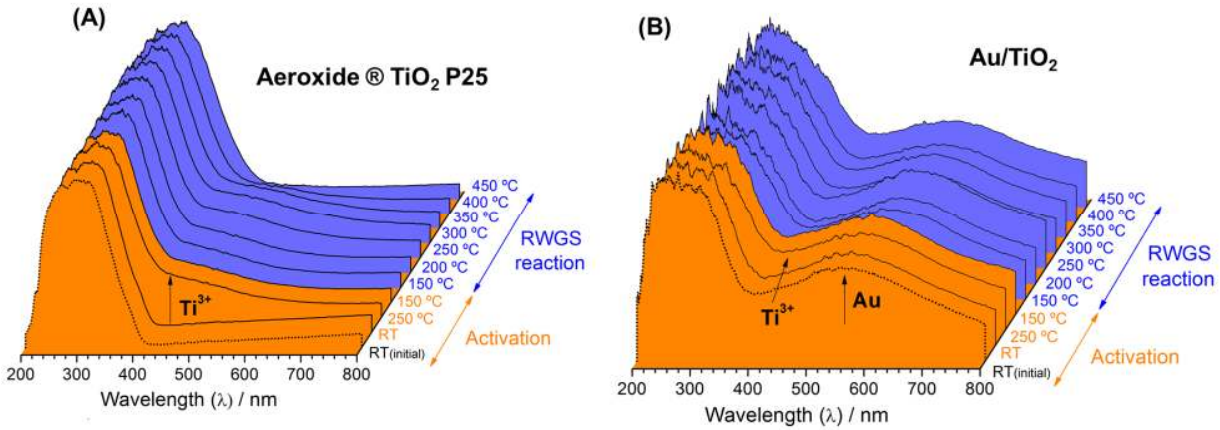

Figure 9. UV-Vis spectra of (A) Aeroxide TiO_2 P25 and (B) Au/TiO_2 catalyst during the activation (50 mL min^{-1} of 10% H_2 in He at 250 ºC for 1 h) and RWGS reaction at 150-450 ºC on the samples

Logically it is expected that Au/TiO_2 presents similar spectral features to those of TiO_2 P25. However, the wide Au plasmon band appearing at around 550 nm renders the identification of spectral features in the 400-800 nm range impossible (Figures 9B). The difference spectra in Figure 10B show contribution of the Au energy levels to titania bandgap changes (the positive band around 350 nm) coupled with the contributions of the titania vacancies formation confirmed by the asymmetric shape of the band toward 450 nm. Higher the temperature, more asymmetrical the shape becomes. This indicates the use of the vacancies created during the reaction (negative contribution appearance tending to increase the asymmetry of the band in the long wavelength range).

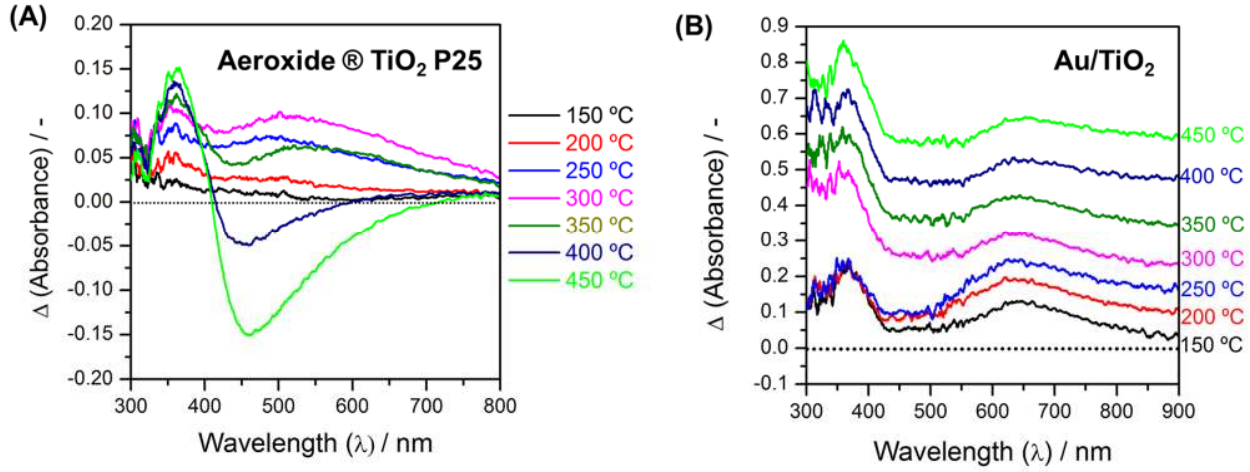

Figure 10. Evolution of difference UV-Vis spectra in function of the RWGS reaction temperature for the samples (A) Aeroxide TiO_2 P25 and (B) Au/TiO_2 catalyst

When the band intensity is compared to the observed CO_2 conversion presented in Figure 2, the increase of the intensity of the band centered at 360 nm is proportional to the RWGS reaction rate as can be observed in Figure 11. This indicates that the catalytic performance of Au/TiO_2 is

correlated with the presence of Ti^{3+}, and consequently with the formation of oxygen vacancies of the support and their concentration.

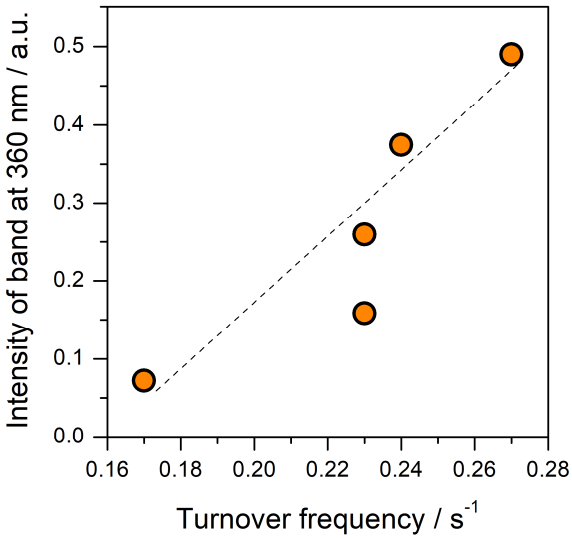

Figure 11. Relationship between the intensity of the UV-Vis band associated to Ti^{3+} and the RWGS reaction rate for Au/TiO_2 catalyst

We can conclude that the oxygen vacancies generated over titania surface directly participates in CO_2 activation generating carbonates species, as also suggested by IR, which are easily reducible to CO and water in presence of hydrogen.

3.4. Oxygen storage complete capacity (OSCC)

According to the *operando* UV-Vis results, the superior performance of Au/TiO_2 catalyst in RWGS reaction can be associated with the increase in the oxygen vacancies concentration of titania. The validation of this affirmation in a quantitative manner generally requires a reasonable measurement of the exact number of oxygen vacancies on the surface and on the gold-support interface. Such estimation is provided by measuring the oxygen storage complete capacity

(OSCC). The obtained results are included in Table 1. TiO_2 P25 is usually considered as oxide with low oxygen mobility and indeed the measured OSCC value is very low and barely influenced by the temperature. The presence of gold, in contrast, boosts significantly the oxygen mobility of titania; almost doubled when the temperature rises from 150 to 250 ºC. At 250 ºC the calculated coefficient for the TiO_x stoichiometry is 1.96 corresponding to maximal titania reduction of around 7 % and suggesting indirectly the presence of Ti^{3+}. This is in a good agreement with the results obtained by *operando* UV-Vis, in which Ti^{3+} species are also detected at this temperature. At 350 ºC the OSCC value decreases which can be tentatively explained by a possible changes in the gold/titanium contact. As detected by TEM (Figure 3) gold nanoparticles sinter during the reaction suggesting diminution of the gold/titanium interface which could reflect in a decrease in the oxygen mobility of titania at this temperature.

Table 1. OSCC properties of TiO_2 support and Au/TiO_2 catalyst at 150, 250 and 350 ºC

Temperature / ºC	OSCC for TiO_2 µmol [O] g^{-1}	OSCC for Au/TiO_2 µmol [O] g^{-1}	Stoichiometric coefficient x for Au/TiO_x	% Surface reducibility on Au/TiO_2
150	10.2	298.4	1.98	4.2
250	11.1	516.6	1.96	7.2
350	12.7	343.6	1.98	4.8

3.5. Discussion of plausible reaction mechanism

Data obtained from *operando* DRIFTS and UV-Vis experiments suggest considerable differences in the prevailing mechanism for the RWGS reaction on Au/Al_2O_3 and Au/TiO_2, respectively.

According to the proposed mechanistic pathways of RWGS reaction over supported noble metal catalysts reported in the literature, two reaction mechanisms have been widely accepted, namely regenerative redox mechanism and associative mechanism with a further possibility that surface formates could be considered intermediates involved in the rate determining step [5]. RWGS reaction proceeds through a concerted pathway where support and gold particles play key roles in the CO_2 activation and the dissociation of H_2.

Our results support that the activation of CO_2 over the two catalysts does not occur *via* direct dissociation of CO_2 to CO and O on the Au particles. In the case of Au/Al_2O_3, CO_2 first reacts with the hydroxyls on alumina to form bicarbonates species. This step does not require the participation of the gold particles [28]. The following steps involve the dissociation of hydrogen over Au and dissociated H atoms can spillover to the support to react with the bicarbonates leading to the formation of formates, which can be decomposed to CO. It has been suggested that this reaction of formation and decomposition of formates preferentially takes place on the interfacial sites between metal and alumina support [30]. Scheme 1 shows this reaction mechanism via formates intermediates proposed for the RWGS reaction on Au/Al_2O_3. Alumina is an irreducible support and thus the absence of oxygen vacancies leads to a decisive role of the hydroxyl groups in the mechanism of the reaction. The participation of hydroxyl groups in the formation and transformation of surface bicarbonates species is fundamental to understand the reaction mechanism on Au/Al_2O_3 catalyst. If we assume that the formation of surface bicarbonates involves hydroxyls groups on the surface then the rate of transformation into formates species will depend also on the surface OH concentration. The H_2 dissociation takes place on the gold particles and the Au-hydride formed reduces the bicarbonate species to adsorbed formate species at the metal-support interface. We propose that the surface formates are initially formed at the Au-support

interface and subsequently decomposed into CO and water. However, they can also migrate to more thermodynamically favourable sites, leading to an accumulation of formates on alumina support. We propose surface formate and bicarbonates species observed by DRIFTS as key intermediates in the RWGS reaction on Au/Al_2O_3. Senayake et al. [39] studied the properties of adsorbed formate on Au(111) using synchrotron-based core level photoemission, near-edge X-ray absorption fine structure (NEXAFS), IR absorption spectroscopy and density functional theory (DFT) calculations. DFT calculations indicate that formic acid can be adsorbed on Au(111) as bidentate formate (0.65 eV) or monodentate formate (0.75 eV). In other DFT study by Mavrikakis and coworkers [48-49] on formic acid decomposition on Au(111) surface, they predicted an energy barrier of 77 kJ mol^{-1} for the C-H cleavage in the Au-bound formate species. A similar value of 75 kJ mol^{-1} was experimentally estimated by Filonenko et al. for the CO_2 hydrogenation on Au/Al_2O_3. On the basis of these considerations, our results of apparent energy activation (79 kJ mol^{-1}) experimentally determined allow us to affirm that the formation and reaction of formates in the metal-support interface is the rate-determining step for the RWGS reaction over Au/Al_2O_3. The amount of formates accumulated on the alumina surface depends markedly on the temperature. According to Meunier et al. [26], the most of formates observed under reaction conditions are spectators, although there are other highly reactive formate species (so-called “fast formates”) whose fraction is enhanced at higher temperature and that are easily observable by transient DRIFTS experiments.

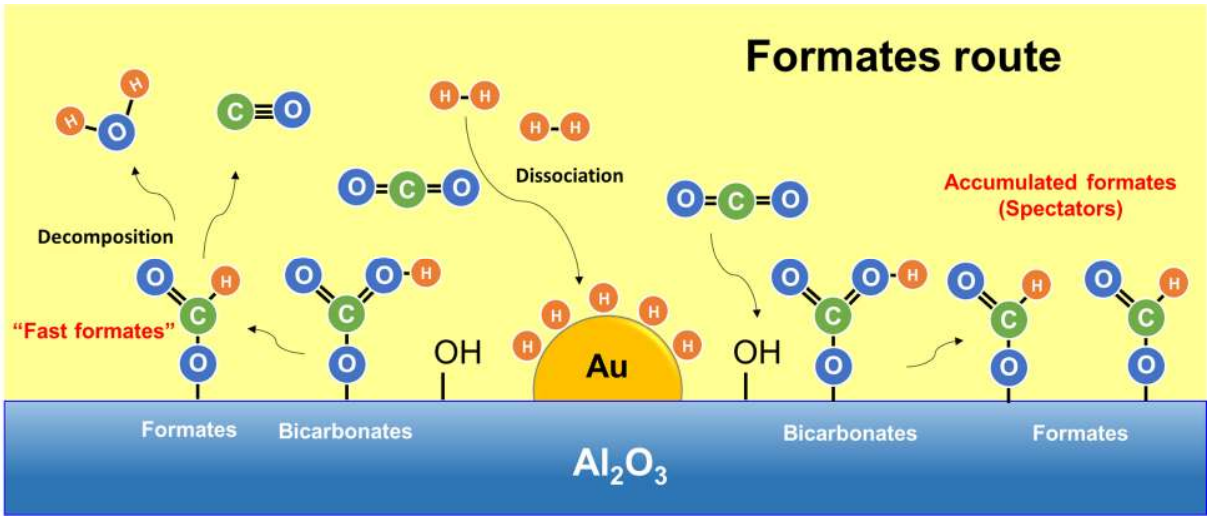

Scheme 1. Proposed mechanism of RWGS reaction for Au/Al_2O_3 catalyst

In the case of Au/TiO_2, titania is a reducible support being able to create oxygen vacancies mainly at the interface metal-support as a consequence of the Shottky function [50]. We identified that there exists a direct correlation between the relative concentration of oxygen vacancies of titania support and the RWGS reaction rate. In general, support oxides containing oxygen vacancies are able to well disperse Au, which leads to excellent catalytic activity [51]. Scheme 2 illustrates the participation of the support in the RWGS mechanism over Au/TiO_2. In accordance to the DRIFTS results, the carbonyls route in which CO_2 is directly dissociated to CO on Au can be ruled out. Rather the carbonates route was suggested as the main pathway to produce gaseous CO. In this route, CO_2 is adsorbed forming surface carbonates that react directly with the oxygen vacancies in the titania, from which CO is released. The results obtained by *operando* UV-Vis also shows that TiO_2 can be reduced in the absence of noble metal facilitating the creation of oxygen vacancies. In a reference catalytic test using titania a low production of CO was observed. The main roles of the gold particles are likely the activation of hydrogen and its subsequent spillover to TiO_2 surface to increase the concentration of oxygen vacancies and thus the number of sites available to react

with CO_2. Goguet et al. [52] proposed a similar mechanism for the RWGS reaction over Pt/CeO_2. They suggested an additional pathway that involves a possible migration of carbonate towards the metal-support interface, where it decomposes via metal-bound carbonyl intermediates. Nevertheless, this route may be discarded in our case since no metal-bound carbonyl was observed. Scheme 2 also includes an additional route associated with the decomposition of formate species on the vacancies, although on the basis of the DRIFTS results it is unlikely that formate is an important intermediate. The carbonates mechanism can be considered a special case of the redox mechanism that involves the formation of a "carbonate-type" intermediate on the support. It implies a direct reaction of CO_2 with the surface oxygen vacancies to form carbonate species and the latter decomposing into CO (g) according to the following elementary reaction steps:

$$CO_2\ (g) + (O^- + \square)\text{-}Ti^{3+} \leftrightarrow [CO_3^-]\text{-}Ti^{4+} \quad (1)$$

$$[CO_3^-]\text{-}Ti^{4+} + Au\text{-}H \leftrightarrow CO\text{-}Ti^{3+} + OH^- \quad (2)$$

$$CO\text{-}Ti^{3+} + OH^- \leftrightarrow CO(g) + H_2O(g) + (O^- + \square)\text{-}Ti^{3+} \quad (3)$$

where □ denotes a surface oxygen vacant site on titania. A similar mechanism was proposed by Kalamaras et al. [53] to explain the reaction mechanism of the WGS over $Pt/Ce_xZr_{1-x}O_2$ catalyst. On the other hand, Rodríguez et al. [54] proposed another mechanism in which the formation of a hydroxycarbonyl (OCOH) intermediates at the gold-titania interface takes place and involves the following steps:

$$H_2\ (g) \leftrightarrow 2H_{ads} \quad (4)$$

$$CO_2\ (g) + H_{ads} \leftrightarrow OCOH_{ads} \quad (5)$$

$OCOH_{ads} \leftrightarrow CO_{ads} + OH_{ads}$ (6)

$OH_{ads} + H_{ads} \leftrightarrow H_2O_{ads}$ (7)

$H_2O_{ads} \leftrightarrow H_2O\ (g)$ (8)

$CO_{ads} \leftrightarrow CO\ (g)$ (9)

The formation of hydroxycarbonyl (OCOH) species is hardly detectable by DRIFTS since these species are very unstable and has a very short lifetime on the gold surface. By means of DFT calculations, Rodríguez et al. [54] predicted that the formation of an OCOH intermediate requires an energy barrier of 0.3 eV in the metal-oxide interface. This barrier is in good agreement with the apparent activation energy obtained for the Arrhenius plot (Figure 4), and it could be assumed that the formation of these intermediate is the rate-limiting step of the reaction with an activation energy of 0.3 eV. In another study, Rodríguez et al. [43] studied the mechanism of CO_2 hydrogenation reaction on Au/TiO_2 and $Au/CeO_x/TiO_2$. They observed high energy barriers for the hydrogenation of CO_2 to HOCO and for the hydrogenation of CO to HCO concluding that the first hydrogenation is the rate-determining step and the presence of vacancies are essential for the binding and conversion of CO_2 in good agreement with our results. Therefore, on Au/TiO_2 catalyst the reaction most probably proceeds through a redox mechanism with the formation of a hydroxylcarbonyl intermediate, which further decomposes to CO and water. The formate or carbonate-like species could be simply spectators bound to oxide support. At higher temperatures, where desorption and/or decomposition of formate and carbonate species will be very fast, we would anticipate that the carbonates/formates routes would become predominant.

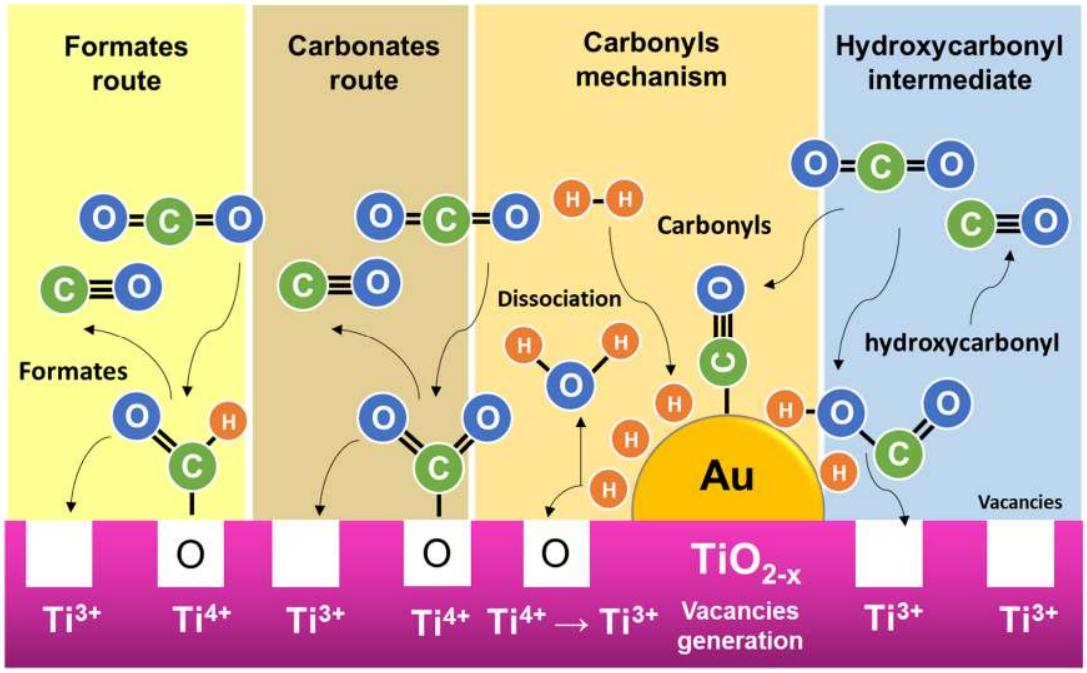

Scheme 2. Proposed mechanism of RWGS reaction for Au/TiO_2 catalyst

In summary, we attribute the difference in the formation rate of CO by RWGS reaction observed for Au/Al_2O_3 and Au/TiO_2 to the presence of oxygen vacancies on TiO_2 able to activate the CO_2 more efficiently. We have demonstrated that the nature of the support has a strong influence on the activity of the catalysts.

4. CONCLUSIONS

The reaction mechanisms of the RWGS reaction over Au/TiO_2 and Au/Al_2O_3 were investigated. DRIFTS results indicate that CO_2 cannot be dissociated to CO directly on the Au particles. The RWGS reaction over Au/Al_2O_3 proceeds *via* formation of formate reaction intermediates that are reduced to produce gaseous CO. In the case of Au/TiO_2 the reaction proceeds at lower temperatures through a redox mechanism with the formation of a hydroxycarbonyl intermediate which further is decomposed to CO and water, where Ti^{3+}, surface hydroxyl, and oxygen vacancies jointly

participate in this route. At higher temperatures, where desorption and/or decomposition of formate and carbonate species occur faster, the carbonates/formates routes would become predominant. The presence of Ti^{3+} and the generation of vacancies of oxygen were confirmed by *operando* UV-Vis spectroscopy, demonstrating the superior performance of Au/TiO_2 in RWGS reaction can be associated with the increase in the concentration of oxygen vacancies in the titania support.

AUTHOR INFORMATION

Corresponding Author

* E-mail: bobadilla@icmse.csic.es

ASSOCIATED CONTENT

Supporting Information

Details on additional characterization data and catalytic performance of the materials

ACKNOWLEDGMENTS

Financial support for this work has been obtained from the Spanish Ministerio de Economía y Competitividad (MINECO) (ENE2013-47880-C3-2-R and ENE2015-66975-C3-2-R). LFB thanks MINECO for the Juan de la Cierva Incorporación 2015 contract. AU thanks the Generalitat de Catalunya for financial support through the CERCA Programme and recognition (2014 SGR 893) and MINECO (CTQ2016-75499-R (AEI/FEDER-UE)) for financial support and support through Severo Ochoa Excellence Accreditation 2014–2018 (SEV-2013-0319).

REFERENCES

(1) Ma, J.; Sun, N.; Zhang, X.; Zhao, N.; Xiao, F.; Wei, W.; Sun, Y., A Short Review of Catalysis for CO_2 Conversion. *Catal. Today* **2009,** *148*, 221-231.

(2) Centi, G.; Perathoner, S., Opportunities and Prospects in the Chemical Recycling of Carbon Dioxide to Fuels. *Catal. Today* **2009,** *148*, 191-205.

(3) Daza, Y. A.; Kuhn, J. N., CO_2 Conversion by Reverse Water Gas Shift Catalysis: Comparison of Catalysts, Mechanisms and Their Consequences for CO_2 Conversion to Liquid Fuels. *RSC Adv.* **2016,** *6*, 49675-49691.

(4) Sakurai, H.; Tsubota, S.; Haruta, M., Hydrogenation of CO_2 over Gold Supported on Metal Oxides. *Appl. Catal. A Gen.* **1993,** *102*, 125-136.

(5) Burch, R., Gold Catalysts for Pure Hydrogen Production in the Water-Gas Shift Reaction: Activity, Structure and Reaction Mechanism. *Phys. Chem. Chem. Phys.* **2006,** *8*, 5483-5500.

(6) Tao, F.; Ma, Z., Water-Gas Shift on Gold Catalysts: Catalyst Systems and Fundamental Studies. *Phys. Chem. Chem. Phys.* **2013,** *15*, 15260-15270.

(7) González-Castaño, M.; Reina, T. R.; Ivanova, S.; Centeno, M. A.; Odriozola, J. A., Pt vs. Au in Water–Gas Shift Reaction. *J. Catal.* **2014,** *314*, 1-9.

(8) Tabakova, T.; Idakiev, V.; Andreeva, D.; Mitov, I., Influence of the Microscopic Properties of the Support on the Catalytic Activity of Au/ZnO, Au/ZrO_2, Au/Fe_2O_3, Au/Fe_2O_3–ZnO, Au/Fe_2O_3–ZrO_2 Catalysts for the WGS Reaction. *Appl. Catal. A Gen.* **2000,** *202*, 91-97.

(9) Tabakova, T.; Ilieva, L.; Ivanov, I.; Zanella, R.; Sobczak, J. W.; Lisowski, W.; Kaszkur, Z.; Andreeva, D., Influence of the Preparation Method and Dopants Nature on the WGS Activity of

Gold Catalysts Supported on Doped by Transition Metals Ceria. *Appl. Catal. B Environ.* **2013,** *136–137*, 70-80.

(10) Jacobs, G.; Ricote, S.; Patterson, P. M.; Graham, U. M.; Dozier, A.; Khalid, S.; Rhodus, E.; Davis, B. H., Low Temperature Water-Gas Shift: Examining the Efficiency of Au as a Promoter for Ceria-Based Catalysts Prepared by CVD of a Au Precursor. *Appl. Catal. A Gen.* **2005,** *292*, 229-243.

(11) Reina, T. R.; Ivanova, S.; Delgado, J. J.; Ivanov, I.; Idakiev, V.; Tabakova, T.; Centeno, M. A.; Odriozola, J. A., Viability of Au/CeO_2–ZnO/Al_2O_3 Catalysts for Pure Hydrogen Production by the Water–Gas Shift Reaction. *ChemCatChem* **2014,** *6*, 1401-1409.

(12) Shekhar, M.; Wang, J.; Lee, W.-S.; Williams, W. D.; Kim, S. M.; Stach, E. A.; Miller, J. T.; Delgass, W. N.; Ribeiro, F. H., Size and Support Effects for the Water–Gas Shift Catalysis over Gold Nanoparticles Supported on Model Al_2O_3 and TiO_2. *J. Am. Chem. Soc.* **2012,** *134*, 4700-4708.

(13) Pakhare, D.; Spivey, J., A Review of Dry (CO_2) Reforming of Methane over Noble Metal Catalysts. *Chem. Soc. Rev.* **2014,** *43*, 7813-7837.

(14) Yang, X.; Kattel, S.; Senanayake, S. D.; Boscoboinik, J. A.; Nie, X.; Graciani, J.; Rodríguez, J. A.; Liu, P.; Stacchiola, D. J.; Chen, J. G., Low Pressure CO_2 Hydrogenation to Methanol over Gold Nanoparticles Activated on a CeO_x/TiO_2 Interface. *J. Am. Chem. Soc.* **2015,** *137*, 10104-10107.

(15) Wang, W.; Wang, S.; Ma, X.; Gong, J., Recent Advances in Catalytic Hydrogenation of Carbon Dioxide. *Chem. Soc. Rev.* **2011,** *40*, 3703-3727.

(16) Ishito, N.; Hara, K.; Nakajima, K.; Fukuoka, A., Selective Synthesis of Carbon Monoxide via Formates in Reverse Water–Gas Shift Reaction over Alumina-Supported Gold Catalyst. *J. Energy Chem.* **2016,** *25*, 306-310.

(17) Millar, G. J.; Rochester, C. H.; Howe, C.; Waugh, K. C., A Combined Infrared, Temperature Programmed Desorption and Temperature Programmed Reaction Spectroscopy Study of CO_2 and H_2 Interactions on Reduced and Oxidized Silica-Supported Copper Catalysts. *Mol. Phys.* **1992,** *76*, 833-849.

(18) Ma, D.; Lund, C. R. F., Assessing High-Temperature Water−Gas Shift Membrane Reactors. *Ind. Eng. Chem. Res.* **2003,** *42*, 711-717.

(19) Tsakoumis, N. E.; York, A. P. E.; Chen, D.; Rönning, M., Catalyst Characterisation Techniques and Reaction Cells Operating at Realistic Conditions; Towards Acquisition of Kinetically Relevant Information. *Catal. Sci. Technol.* **2015,** *5*, 4859-4883.

(20) Sattler, J. J. H. B.; González-Jimenez, I. D.; Mens, A. M.; Arias, M.; Visser, T.; Weckhuysen, B. M., Operando UV-Vis Spectroscopy of a Catalytic Solid in a Pilot-Scale Reactor: Deactivation of a CrO_x/Al_2O_3 Propane Dehydrogenation Catalyst. *Chem. Commun.* **2013,** *49*, 1518-1520.

(21) *https://secure.strem.com/catalog/family/Aurolite/* (access date: 2013/06/15)

(22) Ovsitser, O.; Cherian, M.; Brückner, A.; Kondratenko, E. V., Dynamics of Redox Behavior of Nano-Sized VO_x Species Over Ti–Si-MCM-41 from Time-Resolved In Situ UV/Vis Analysis. *J. Catal.* **2009,** *265*, 8-18.

(23) Kondratenko, E. V.; Takahashi, N.; Nagata, N.; Ibe, M.; Hirata, H.; Takahashi, H., Operando UV/Vis Analysis of the Synergy Effect between Copper and Gold in Nitric Oxide Reduction over Gold and Copper on Aluminacatalysts. *ChemCatChem* **2015,** *7*, 3956-3962.

(24) Walther, G.; Mowbray, D. J.; Jiang, T.; Jones, G.; Jensen, S.; Quaade, U. J.; Horch, S., Oxidation of CO and H_2 by O_2 and N_2O on Au/TiO_2 Catalysts in Microreactors. *J. Catal.* **2008,** *260*, 86-92.

(25) Jacobs, G.; Patterson, P. M.; Williams, L.; Chenu, E.; Sparks, D.; Thomas, G.; Davis, B. H., Water-Gas Shift: In Situ Spectroscopic Studies of Noble Metal Promoted Ceria Catalysts for CO Removal in Fuel Cell Reformers and Mechanistic Implications. *Appl. Catal. A Gen.* **2004,** *262*, 177-187.

(26) Meunier, F. C.; Reid, D.; Goguet, A.; Shekhtman, S.; Hardacre, C.; Burch, R.; Deng, W.; Flytzani-Stephanopoulos, M., Quantitative Analysis of the Reactivity of Formate Species seen by DRIFTS over a $Au/Ce(La)O_2$ Water–Gas Shift Catalyst: First Unambiguous Evidence of the Minority Role of Formates as Reaction Intermediates. *J. Catal.* **2007,** *247* (2), 277-287.

(27) Boccuzzi, F.; Chiorino, A.; Manzoli, M.; Andreeva, D.; Tabakova, T., FTIR Study of the Low-Temperature Water–Gas Shift Reaction on Au/Fe_2O_3 and Au/TiO_2 Catalysts. *J. Catal.* **1999,** *188*, 176-185.

(28) Szanyi, J.; Kwak, J. H., Dissecting the Steps of CO_2 reduction: 1. The Interaction of CO and CO_2 with γ-Al_2O_3: an In Situ FTIR Study. *Phys. Chem. Chem. Phys.* **2014,** *16*, 15117-15125.

(29) Trillo, J. M.; Munuera, G.; Criado, J. M., Catalytic Decomposition of Formic Acid on Metal Oxides. *Catal. Rev.* **1972,** *7*, 51-86.

(30) Wang, X.; Shi, H.; Kwak, J. H.; Szanyi, J., Mechanism of CO_2 Hydrogenation on Pd/Al_2O_3 Catalysts: Kinetics and Transient DRIFTS-MS Studies. *ACS Catal.* **2015,** *5*, 6337-6349.

(31) Wang, X.; Hong, Y.; Shi, H.; Szanyi, J., Kinetic Modeling and Transient DRIFTS–MS Studies of CO_2 Methanation over Ru/Al_2O_3 Catalysts. *J. Catal.* **2016,** *343*, 185-195.

(32) Gaur, S.; Wu, H.; Stanley, G. G.; More, K.; Kumar, C. S. S. R.; Spivey, J. J., CO Oxidation Studies over Cluster-derived Au/TiO_2 and AUROlite™ Au/TiO_2 Catalysts using DRIFTS. *Catal. Today* **2013,** *208*, 72-81.

(33) Denkwitz, Y.; Zhao, Z.; Hörmann, U.; Kaiser, U.; Plzak, V.; Behm, R. J., Stability and Deactivation of Unconditioned Au/TiO_2 Catalysts during CO Oxidation in a Near-Stoichiometric and O_2-Rich Reaction Atmosphere. *J. Catal.* **2007,** *251*, 363-373.

(34) Bando, K. K.; Sayama, K.; Kusama, H.; Okabe, K.; Arakawa, H., In-Situ FT-IR Study on CO_2 Hydrogenation over Cu Catalysts Supported on SiO_2, Al_2O_3, and TiO_2. *Appl. Catal. A Gen.* **1997,** *165*, 391-409.

(35) Nomura, N.; Tagawa, T.; Goto, S., In Situ FTIR Study on Hydrogenation of Carbon Dioxide over Titania-Supported Copper Catalysts. *Appl. Catal. A Gen.* **1998,** *166*, 321-326.

(36) Baltrusaitis, J.; Jensen, J. H.; Grassian, V. H., FTIR Spectroscopy Combined with Isotope Labeling and Quantum Chemical Calculations to Investigate Adsorbed Bicarbonate Formation following Reaction of Carbon Dioxide with Surface Sydroxyl Groups on Fe_2O_3 and Al_2O_3. *J. Phys. Chem. B* **2006,** *110*, 12005-12016.

(37) Fottinger, K.; Schlögl, R.; Rupprechter, G., The Mechanism of Carbonate Formation on Pd-Al_2O_3 Catalysts. *Chem. Commun.* **2008,** 3, 320-322.

(38) Guglielminotti, E.; Giamello, E.; Pinna, F.; Strukul, G.; Martinengo, S.; Zanderighi, L., Elementary Steps in CO Hydrogenation on Rh Catalysts Supported on ZrO_2 and Mo/ZrO_2. *J. Catal.* **1994,** *146*, 422-436.

(39) Senanayake, S. D.; Stacchiola, D.; Liu, P.; Mullins, C. B.; Hrbek, J.; Rodriguez, J. A., Interaction of CO with OH on Au(111): HCOO, CO_3, and HOCO as Key Intermediates in the Water-Gas Shift Reaction. *J. Phys. Chem. C* **2009,** *113*, 19536-19544.

(40) Gokhale, A. A.; Dumesic, J. A.; Mavrikakis, M., On the Mechanism of Low-Temperature Water Gas Shift Reaction on Copper. *J. Am. Chem. Soc.* **2008,** *130*, 1402-1414.

(41) Deiana, C.; Fois, E.; Coluccia, S.; Martra, G., Surface Structure of TiO_2 P25 Nanoparticles: Infrared Study of Hydroxyl Groups on Coordinative Defect Sites. *J. Phys. Chem. C* **2010,** *114*, 21531-21538.

(42) Bitter, J. H.; Seshan, K.; Lercher, J. A., Mono and Bifunctional Pathways of CO_2/CH_4 Reforming over Pt and Rh based Catalysts. *J. Catal.* **1998,** *176*, 93-101.

(43) Rodriguez, J. A.; Liu, P.; Stacchiola, D. J.; Senanayake, S. D.; White, M. G.; Chen, J. G., Hydrogenation of CO_2 to Methanol: importance of Metal–Oxide and Metal–Carbide Interfaces in the Activation of CO_2. *ACS Catal.* **2015,** *5*, 6696-6706.

(44) Raskó, J., FTIR Study of the Photoinduced Dissociation of CO_2 on Titania-Supported Noble Metals. *Catal. Lett.* **1998,** *56*, 11-15.

(45) Liu, H.; Ma, H. T.; Li, X. Z.; Li, W. Z.; Wu, M.; Bao, X. H., The Enhancement of TiO_2 Photocatalytic Activity by Hydrogen Thermal Treatment. *Chemosphere* **2003,** *50*, 39-46.

(46) Xiong, L.-B.; Li, J.-L.; Yang, B.; Yu, Y., Ti^{3+} in the Surface of Titanium Dioxide: Generation, Properties and Photocatalytic Application. *J. Nanomater.* **2012,** *2012*, 5-8.

(47) Kuznetsov, V. N.; Serpone, N., Visible Light Absorption by Various Titanium Dioxide Specimens. *J. Phys. Chem. B* **2006,** *110*, 25203-25209.

(48) Carrasquillo-Flores, R.; Singh, S.; Li, S.; Alba-Rubio, A. C.; Dumesic, J. A.; Mavrikakis, M. In *Formic acid decomposition on Au catalysts: Identifying the active site for improved catalyst design*, Catalysis and Reaction Engineering Division 2014 - Core Programming Area at the 2014 AIChE Annual Meeting, **2014**; p 450.

(49) Singh, S.; Li, S.; Carrasquillo-Flores, R.; Alba-Rubio, A. C.; Dumesic, J. A.; Mavrikakis, M., Formic acid decomposition on Au catalysts: DFT, microkinetic modeling, and reaction kinetics experiments. *AIChE J.* **2014,** *60* (4), 1303-1319.

(50) Frost, J. C., Junction Effect Interactions in Methanol Synthesis Catalysts. *Nature* **1988,** *334*, 577-580.

(51) Hernández, W. Y.; Romero-Sarria, F.; Centeno, M. A.; Odriozola, J. A., In Situ Characterization of the Dynamic Gold−Support Interaction over Ceria Modified Eu^{3+}. Influence of the Oxygen Vacancies on the CO Oxidation Reaction. *J. Phys. Chem. C* **2010,** *114*, 10857-10865.

(52) Goguet, A.; Meunier, F. C.; Tibiletti, D.; Breen, J. P.; Burch, R., Spectrokinetic Investigation of Reverse Water-Gas-Shift Reaction Intermediates over a Pt/CeO_2 Catalyst. *J. Phys. Chem. B* **2004,** *108*, 20240-20246.

(53) Kalamaras, C. M.; Dionysiou, D. D.; Efstathiou, A. M., Mechanistic Studies of the Water–Gas Shift Reaction over $Pt/Ce_xZr_{1-x}O_2$ Catalysts: The Effect of Pt Particle Size and Zr Dopant. *ACS Catal.* **2012,** *2*, 2729-2742.

(54) Rodríguez, J. A.; Evans, J.; Graciani, J.; Park, J.-B.; Liu, P.; Hrbek, J.; Sanz, J. F., High Water−Gas Shift Activity in TiO_2(110) Supported Cu and Au Nanoparticles: Role of the Oxide and Metal Particle Size. *J. Phys. Chem. C* **2009,** *113*, 7364-7370.

SYNOPSIS (TOC)

SUPPORTING INFORMATION

Unravelling the Role of Oxygen Vacancies in the Mechanism of the Reverse Water-Gas-Shift Reaction by Operando DRIFTS and UV-Vis Spectroscopy

Luis F. Bobadilla †,, José L. Santos †, Svetlana Ivanova †, José A. Odriozola † and Atsushi Urakawa ‡*

† Instituto de Ciencia de Materiales de Sevilla, Centro Mixto CSIC-Universidad de Sevilla, Av. Américo Vespucio 49, 41092 Sevilla, Spain

‡ Institute of Chemical Research of Catalonia (ICIQ), The Barcelona Institute of Science and Technology, Av. Països Catalans 16, 43007 Tarragona, Spain

(*) Corresponding author: bobadilla@icmse.csic.es

EXPERIMENTAL DETAILS

X-ray diffraction (XRD) measurements were performed on an X'Pert Pro PANalytical diffactometer. Diffraction patterns were recorded using Cu Kα radiation (40 mA, 45 kV) over a 10–90° 2Θ-range and a position-sensitive detector using a step size of 0.05° and a step time of 240 s.

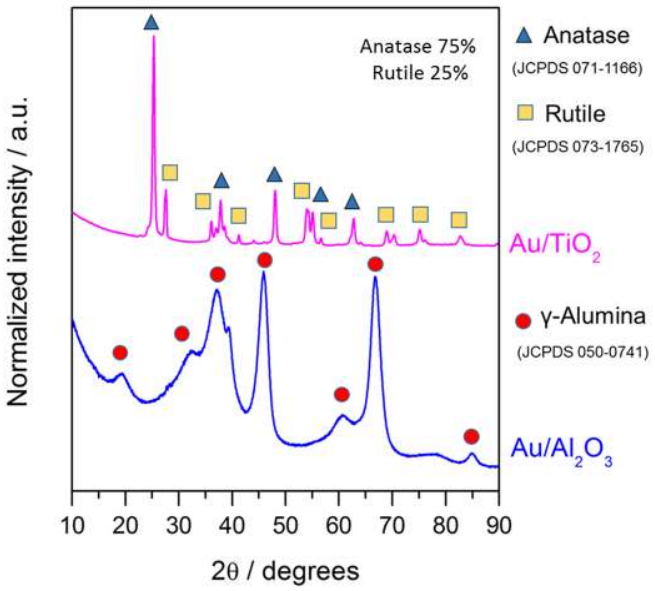

Figure S1. XRD patterns of Au/Al_2O_3 and Au/TiO_2

Due to the observed variations in the gold particle size of both catalysts during the RWGS reaction, the catalytic activity was also evaluated in terms of conversion up/down curves. As example, we have included in Fig. S2 the obtained results for Au/TiO_2 catalyst under kinetic regime conditions at GHSV = 40,000 h^{-1}. As can be observed the conversion up/down is identical even reaching maximal temperature of 400 ºC (Fig. S2A) and one can guarantee that Ea is not under-estimated (Fig. S2B).

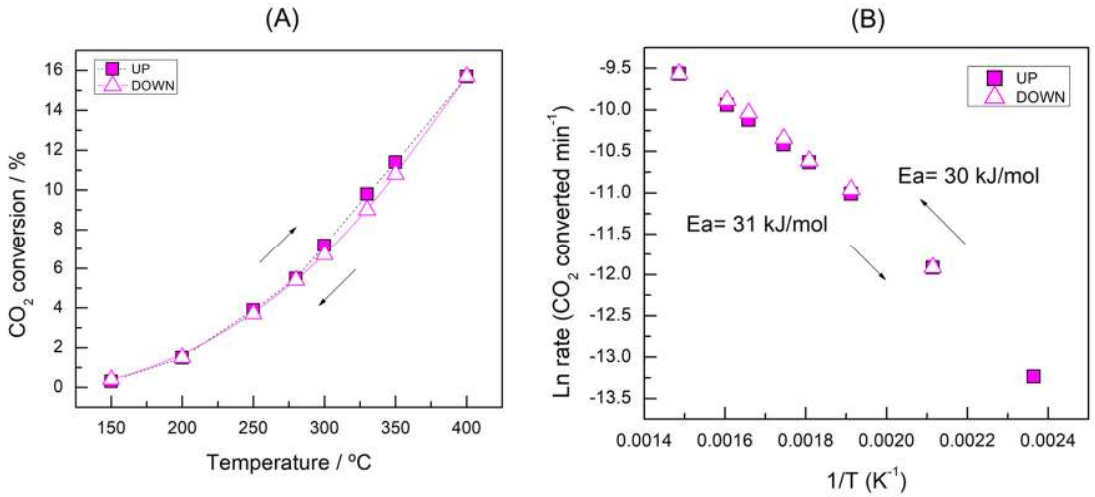

Figure S2. (A) Conversion up-down curves and (B) Arrhenius plot for the Au/TiO_2 catalysts in RWGS reaction. Reaction conditions: GHSV = 40,000 h^{-1} and H_2/CO_2 molar ratio = 4